Engineered Science
DOI: https://dx.doi.org/10.30919/es1482

Selective Sorption of Gold Ions from Iron-Rich Solutions Using a Dual-Phase Interpolymer System

Talkybek Jumadilov,[1,2] Meruyert Suleimenova[1,2,*] and Juozas Vidas Gražulevičius[3]

Abstract

This study investigates the selective sorption of gold(I) ions from binary gold-iron solutions using the interpolymer system Amberlite IR120:AV-17-8. The system leverages remote interactions between cationic and anionic resins to enhance gold selectivity. Amberlite IR120 (H^+ form) and AV-17-8 (OH^- form) were evaluated at molar ratios of 6:0, 5:1, 4:2, 3:3, 2:4, 1:5, and 0:6. Sorption characteristics were analyzed using gravimetry, inductively coupled plasma optical emission spectroscopy, Fourier transform infrared spectroscopy, thermogravimetric analysis and scanning electron microscopy. The optimized 4:2 ratio exhibited the highest gold selectivity, achieving 96.26% sorption after 48 hours, while iron sorption remained at 42.33%. In contrast, Amberlite IR120 (6:0) showed negligible sorption (~3%), whereas AV-17-8 (0:6) reached 91.9% for gold and 92.33% for iron. Desorption with 9% thiourea and 2% sulfuric acid yielded 92.28% gold recovery and 46.44% iron recovery at the 4:2 ratio, which correlates with the high sorption efficiency. Based on calculations per mole of anion exchanger, the highest gold sorption was 18.45 mg/L at a 5:1 ratio, 301% higher than the 4.60 mg/L at a 0:6 ratio and gold desorption peaked at 15.4 mg/L at a 5:1 ratio, 266.67% higher than the 4.20 mg/L at a 0:6. These findings demonstrate that optimizing cation-anion ratios significantly enhances gold recovery. The system's efficiency is attributed to remote interactions and enhanced ion exchange, as analyzed using Pearson's Hard and Soft Acids and Bases theory.

Keywords: Gold ions; Iron ions; Interpolymer system; Remote interaction effect; Sorption kinetics.
Received: 22 October 2024; Revised: 28 February 2025; Accepted: 31 March 2025.
Article type: Research article.

1. Introduction

Gold is a precious metal with a wide range of applications and is renowned for its unique physicochemical properties, including excellent thermal and electrical conductivities, remarkable ductility, chemical inertness, and exceptional corrosion resistance.[1-4] These properties make gold an invaluable material across various industries, sustaining a continuous and growing demand for its production. However, the finite availability of gold resources and the complexity of extracting gold from low-grade ores necessitate the development of more efficient and cost-effective recovery methods.[5] The sorption and refining of high-purity gold are always fraught with significant challenges due to the complex composition of gold-bearing ores, which often contain other metals such as copper, silver, zinc, and iron.[6,7] The presence of associated metals not only complicates the separation process but also increases the likelihood of resource wastage and environmental degradation. Consequently, the sorption of gold from both natural ores and secondary sources remains a critical task in modern metallurgy.[8-12] The increasing heterogeneity of ore composition further emphasizes the need to develop advanced methods capable of efficiently separating and recovering gold while mitigating the interference of accompanying elements in the gold sorption process.

Over the years, various methods have been developed for gold sorption, including gravity separation,[13,14] flotation,[15-18] amalgamation,[19-21] heap leaching,[22-25] bioleaching.[26-29] The selection of the appropriate process is primarily determined by

[1] *Bekturov Institute of Chemical Sciences, 106 Sh. Ualikhanov Str., Almaty, 050010, Kazakhstan*
[2] *Faculty of Natural Sciences and Geography, Abai Kazakh National Pedagogical University, 13 Dostyk Ave., Almaty, 050010, Kazakhstan*
[3] *Department of Polymer Chemistry and Technology, Kaunas University of Technology, 73 K. Donelaičio Street, Kaunas, 44249, Lithuania*
**Email:* suleimenova.me@gmail.com (M. Suleimenova)

the ore's mineralogical properties and the concentration of gold it contains. Among these techniques, cyanidation remains one of the most widely employed processes, particularly for treating low-grade ores due to its ability to extract gold efficiently from ores with low concentrations. This makes cyanidation especially valuable in large-scale operations where alternative methods may not be economically viable. However, despite its effectiveness, this method raises concerns about environmental contamination and safety, particularly regarding the interaction and complexation with cyanide and its disposal.[30-33] Cyanide leaching involves the complexation of gold with cyanide ions in an alkaline solution in the presence of oxygen, as illustrated by the reaction shown in Equation (1):[34,35]

$$4Au + 8CN^- + O_2 + 2H_2O \rightarrow 4[Au(CN)_2]^- + 4OH^- \quad (1)$$

While the cyanidation process effectively leaches gold into solution, the subsequent separation of gold from the resulting cyanide complexes poses significant challenges, particularly in the presence of accompanying metal ions. Recently, flotation has emerged as a promising approach for improving gold recovery, particularly through the use of superhydrophobic materials. One effective strategy in this field involves enhancing flotation performance by incorporating superhydrophobic magnetic carriers (SMC). This method, known as SMC-based carrier flotation, has demonstrated high efficiency in recovering fine mineral particles from complex ores.[36] Moreover, superhydrophobic materials are widely applied in various industries due to their ability to improve selectivity, recovery rates, cost-effectiveness, and wettability control.[37-39] These advancements underscore the growing interest in flotation-based techniques as a viable and sustainable alternative for metal extraction.

Despite advances in hydrometallurgy, the issue of improving the selectivity and efficiency of sorbents for gold sorption remains relevant.[8] Adsorption methods using various materials such as hydrogels,[40-42] ion exchange resins,[43-46] biological adsorbents,[47,48] functionalized magnetic chitosan nanoparticles,[49,50] and activated carbons have garnered significant attention due to their role in extracting various metal ions from aqueous media.[51-53] Hydrogels, particularly those based on N,N-dimethylacrylamide (DMAA), have been widely explored for their ability to adsorb heavy metal ions from aqueous solutions due to their high swelling capacity and functional groups that facilitate metal binding.[54,55] These materials demonstrate considerable potential in enhancing metal recovery, offering solutions aimed at increasing the efficiency and sustainability of sorption processes.[56-58] While these advanced materials offer promising approaches for improving gold sorption, conventional technologies such as carbon-in-leach and carbon-in-pulp remain the most widely used in industrial practice. However, their efficiency is often reduced when processing carbonaceous ores exhibiting preg-robbing behavior. In such ores, naturally occurring organic carbon competes with the sorbent for gold cyanide complexes, significantly reducing the performance of activated carbon.

Recent studies have shown that protonated activated carbon in the carbon-in-leach process effectively mitigates the preg-robbing effect associated with carbonaceous ores. Due to improved adsorption properties over conventional sorbents, protonated activated carbon enhances gold recovery and reduces metal losses during processing.[59] An alternative approach involves resin-in-leach technology, which utilizes ion-exchange resins with high selectivity for gold and has demonstrated promising results under similar processing conditions. At the Penjom plant in Malaysia, replacing activated carbon with a strong-base anion exchange resin increased gold recovery to 90% and reduced sorbent losses to less than 5 g/t of ore.[60] However, the widespread industrial adoption of resin-in-leach is often constrained by the high cost of specialized resins such as Minix or Purogold. This economic factor presents a challenge for long-term viability, particularly in operations with fluctuating ore compositions
In contrast, the Amberlite IR120:AV-17-8 interpolymer system offers a cost-effective and technically robust alternative. With commercially available prices of approximately 2.0 USD/kg for AV-17-8 and 2.5 USD/kg for Amberlite IR120, the system combines cationic and anionic exchange functionalities to achieve enhanced sorption performance via synergistic interaction. Furthermore, the system demonstrates high resistance to organic fouling, making it suitable for use in conjunction with blanking agents and under complex leaching conditions commonly encountered in preg-robbing ores.

Considering the strengths of these works, our research has focused on developing interpolymer systems that combine different ion exchange resins to enhance the efficiency of metal ion recovery. Specifically, the use of an interpolymer system consisting of ion exchangers such as Amberlite IR120 and AV-17-8 allows for significantly improved adsorption of gold ions. The primary objective of this research was to investigate the selective sorption capabilities of this system for the recovery of Au(I) ions from complex solutions containing both gold and iron ions. By exploring various molar ratios (X:Y) of the Amberlite IR120 cation exchange resin and the AV-17-8 anion exchange resin at different interaction times,

we aim to enhance the system's selectivity and efficiency in gold recovery, thereby contributing to the advancement of more sustainable and effective methods for precious and other metal sorption.

2. Experimental section

2.1 Materials and equipment

The strongly acidic cation exchanger Amberlite IR120 (H^+ form) (Lenntech, Delfgauw, The Netherlands), a gel-type resin based on sulfonated styrene-divinylbenzene copolymer (600-800 µm granule size), and the strongly basic anion exchanger AV-17-8 (OH^- form) (Azot, Cherkasy, Ukraine), a gel-type resin composed of styrene-divinylbenzene copolymer (315–1250 µm granule size), were employed. Potassium dicyanoaurate(I) ($KAu(CN)_2$) and potassium hexacyanoferrate(II) trihydrate ($K_4[Fe(CN)_6]\cdot 3H_2O$) (Sigma-Aldrich, Darmstadt, Germany) were used to prepare the model solution with controlled concentrations of gold and iron to ensure experimental precision. Desorption was performed using a 9% thiourea and 3% sulfuric acid solution, which facilitated the formation of a positively charged thiocarbamide complex $\{Au[CS(NH_2)_2]\}^+$, as shown in Equation (2):

$$RAu(CN)_2 + 2CS(NH_2)_2 + H_2SO_4 \rightarrow R_2SO_4 + Au[SC(NH_2)_2]_2SO_4 + 2HCN \quad (2)$$

All reagents were of analytical grade, and deionized water was used throughout.

The mass measurements of the ion exchangers were conducted using a Shimadzu AY220 analytical balance (Shimadzu Corporation, Kyoto, Japan) with high precision. Residual gold and iron concentrations in the solution were measured using an inductively coupled plasma optical emission spectrometry (ICP-OES) spectrometer (ICAP PRO XP, Thermo Fisher Scientific, Winsford, UK), with a wavelength range of 167.021 to 852.145 nm, ensuring a measurement error below 1%. Polymer analyses included Fourier transform infrared (FTIR) spectroscopy for functional group identification, thermogravimetric analysis (TGA) for thermal behavior, and scanning electron microscopy (SEM) to assess the distribution of gold ions on the polymer surfaces.

2.2 Preparation and formation of the interpolymer system "Amberlite IR120:AV-17-8" (X:Y)

To develop an effective interpolymer system capable of remote interaction in aqueous media, the selection of polymers with appropriate chemical properties to ensure high sorption capacity is essential. Amberlite IR120 and AV-17-8 were chosen due to their extensively studied sorption characteristics, broad applicability in ion exchange processes, availability, and cost-effectiveness. Despite their extensive use, the behavior of these ion exchangers within an interpolymer system, particularly with regard to gold ions, has not been comprehensively explored. The preparation of the interpolymer system involved the following steps:

1. Each ion-exchange resin was precisely weighed to ensure consistency across experiments. The total amount of ion exchange resin in each setup was kept constant at 6 moles, with varying molar ratios of Amberlite IR120 and AV-17-8.
2. The weighed samples of Amberlite IR120 and AV-17-8 were placed in specially designed polypropylene cells with pore sizes of 100 µm. These pores allow free ion exchange while keeping the ion exchanger particles in place.
3. Fig. 1 shows the experimental setup, which included polypropylene cells containing the cation and anion exchangers positioned 2 cm apart. This spatial separation facilitates the remote interaction between the resins in the aqueous medium.
4. The interpolymer system was formed by placing the polypropylene cells with Amberlite IR120 and AV-17-8 together into a single beaker containing the model solution. The molar ratios of the resins were varied (6:0, 5:1, 4:2, 3:3, 2:4, 1:5, and 0:6), while keeping the total amount of ion-exchange material constant at 6 moles in each setup.

2.3 The mechanism of polymer interaction in an interpolymer system "Amberlite IR120:AV-17-8" (X:Y)

Amberlite IR120, in its H^+ form, acts as a strong acid due to the presence of sulfonic acid groups ($-SO_3H$) introduced through the sulfonation of a styrene-divinylbenzene copolymer. These functional groups enable Amberlite IR120 to act as a proton (H^+) donor in an aqueous solution, a characteristic feature of strong acid cation exchange resins (Scheme 1). Conversely, AV-17-8, in its OH^- form, functions as a strong base, with quaternary ammonium groups acting as hydroxide ion (OH^-) donors in solution, typical of strong base anion exchange resins (Scheme 2). The remote interaction between these two resins in an aqueous environment results in the formation of weakly dissociated water molecules, which subsequently activate and stabilize the functional groups of the polyelectrolytes. This activation enhances the local concentration of H_3O^+ and OH^- ions around the ion exchangers, thereby promoting the dissociation of counter ions within the system. As shown in Scheme 3, the positively charged ammonium groups (N^+) interact with the negatively charged $[Au(CN)_2]^-$ anion, forming a stable ion pair. This electrostatic attraction effectively binds the gold complex to the anion exchange resin, contributing to enhanced sorption capacity.

The primary mechanism behind the system's high selectivity and sorption efficiency is the increased dissociation

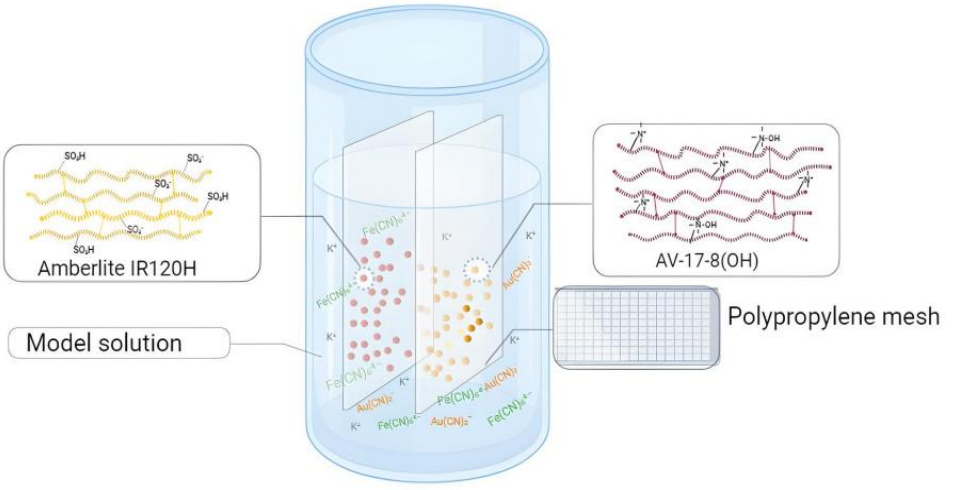

Fig. 1: Illustration of the interpolymer system "Amberlite IR120H:AV-17-8" (X:Y) in an aqueous medium.

and ionization, which elevates the concentration of positively charged ions on the AV-17-8 resin. This intensified electrostatic interaction with the $[Au(CN)_2]^-$ complex significantly improves gold sorption, enhancing the overall performance of the interpolymer system. The behavior of ion exchange groups within this system can be further explained by Pearson's Hard and Soft Acids and Bases (HSAB) theory.[61] According to this theory, the interaction between a hard acid, such as H^+, and a hard base, like OH^-, leads to the formation of water molecules, which play a crucial role in activating and stabilizing ion exchanger functional groups.[62] This activation is particularly evident in systems containing Amberlite IR120 and AV-17-8, where localized increases in H_3O^+ and OH^- concentrations are observed near the ion exchanger surfaces. Such ionic gradients can alter the distribution of neutral water molecules, reducing their availability within the interpolymer matrix compared to their individual use. This altered water distribution can influence sorption efficiency, as the availability of neutral water molecules affects hydration and subsequent ion exchange processes. Cooperative interactions between the ion exchangers in the interpolymer system led to more effective ion separation and recovery, demonstrating the relevance of HSAB theory in understanding complex behaviors in ion exchange systems.

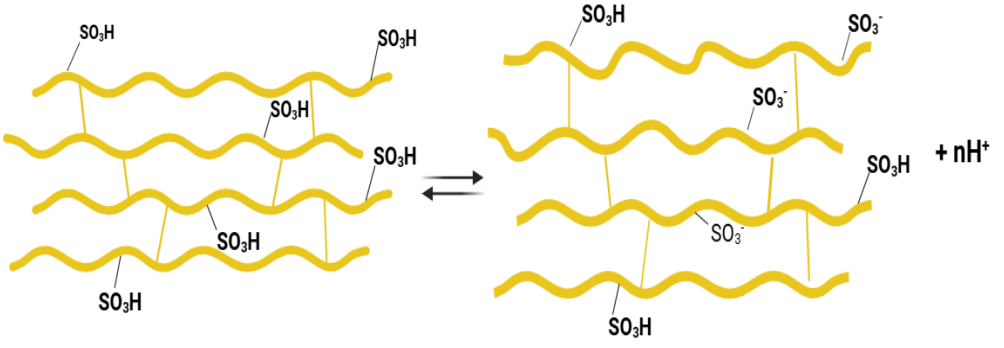

Scheme 1: The dissociation of Amberlite IR120(H^+) ion exchanger in aqueous solution.

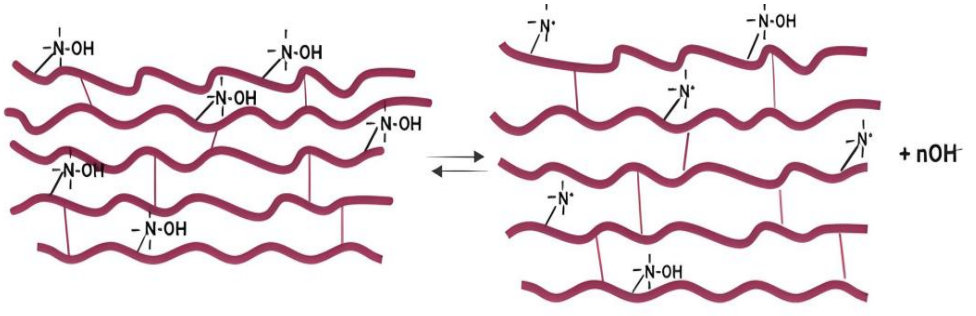

Scheme 2: The dissociation of AV-17-8 ion exchanger in aqueous solution.

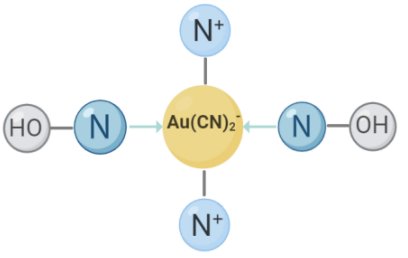

Scheme 3: Interaction between the $[Au(CN)_2]^-$ anion complex and ammonium groups of the AV-17-8 ion exchange resin.

2.4 Sorption procedure for Au(I) and Fe(II) ions

A model solution containing gold and iron ions was prepared by dissolving potassium dicyanoaurate ($KAu(CN)_2$) and potassium hexacyanoferrate (II) trihydrate ($K_4[Fe(CN)_6]\cdot 3H_2O$) to achieve a concentration of 30 mg/L for each ion. This solution was used to evaluate the sorption capacity of the interpolymer system. The experiment was conducted over 48 hours to fully analyze sorption and determine key kinetic parameters. Aliquots of 2 mL were taken at predetermined intervals (1 hour, 2.5 hours, 6 hours, 24 hours, and 48 hours), with a total of 35 aliquots collected. The choice of these time intervals was based on preliminary experiments, which demonstrated significant electrochemical and conformational changes in the polymers of the interpolymer system during these periods. The experiment was repeated three times to ensure reproducibility and accuracy of the results.

The residual concentrations of Au(I) and Fe(II) ions in the aliquots were measured using ICP-OES, a precise method for determining metal ion concentrations in aqueous solutions. For ICP-OES analysis, the aliquots were diluted 5-fold to establish optimal measurement conditions. Gold concentrations were recorded at a wavelength of 242.795 nm, while iron concentrations were measured at 239.562 nm, ensuring high analytical sensitivity and reliability of the data. This enabled an accurate assessment of the metal ions absorbed by the interpolymer system, offering valuable insight into its sorption efficiency. The sorption degree (η) was calculated using Equation (3):

$$\eta = \frac{C_{initial} - C_{residual}}{C_{initial}} \times 100\% \quad (3)$$

where $C_{initial}$ and $C_{residual}$ are the initial and residual concentrations (in g/L) of Au(I) and Fe(II) ions in solutions, respectively.

2.5 Desorption procedure for Au(I) and Fe(II) ions

To examine desorption, a solution of 9% thiourea and 2% sulfuric acid was prepared and used as the eluent. The desorption process was conducted over 72 hours, with aliquots collected at 0.5, 2.5, 6, 24, 48, and 72 hours. Desorbed ion concentrations were determined using ICP-OES. This desorption study revealed varying efficiencies depending on the polymer ratios used. The desorption degree (R) was calculated by Equation (4):

$$R = \frac{m_{desorbed}}{m_{sorbed}} \times 100\% \quad (4)$$

where $m_{desorbed}$ is the mass of ions desorbed from the interpolymer system and m_{sorbed} is the mass of ions initially sorbed onto the system (mg/L).

2.6 Determination of polymer chain binding degree (θ) and effective dynamic exchange capacity (Q) for Au(I) and Fe(II) ions

The polymer chain binding degree (θ) of the ion-exchange resins serves as a quantitative measure of the effectiveness of the interaction between Amberlite IR120 and AV-17-8 with ions within the polymer matrix. This degree reflects the number of polymer units involved in forming chemical bonds or complexes with the target ions. The binding degree was calculated using Equation (5), allowing for the quantification of the polymer chains' affinity for Au(I) ions and the overall efficiency of the ion-exchange process within the interpolymer system.

$$\theta = \frac{\vartheta_{sorbed}}{\vartheta_1 + \vartheta_2} \times 100\ \% \quad (5)$$

where ϑ_{sorbed} is the absorbed Au(I) and Fe(II) ions (in mol), ϑ_1 is the amount of Amberlite IR120 (mol), and ϑ_2 is the amount of AV-17-8 (mol).

The effective dynamic exchange capacity (Q) of the ion-exchange resins quantifies the efficiency of the interaction between Amberlite IR120 and AV-17-8 with ions within the polymer matrix. This parameter represents the number of ion-exchange groups actively participating in the ion exchange process, providing insight into the polymers' ability to effectively extract target ions from the solution. The effective dynamic exchange capacity was determined in Equation (6):

$$Q = \frac{\vartheta_{sorbed}}{m_{sorbent}} \quad (6)$$

where ϑ_{sorbed} is the absorbed Au(I) and Fe(II) ions (mmol), and $m_{sorbent}$ is the mass of sorbent (g).

3. Results and discussion

3.1 Selective sorption of gold ions from gold-iron containing solution by the interpolymer system "Amberlite IR120:AV-17-8" (X:Y)

The change in the concentration of Au(I) and Fe(II) ions during sorption by the interpolymer system "Amberlite IR120:AV-17-8" (X:Y) is depicted in Fig. 2. In the first 2.5 hours, significant sorption activity was observed across different molar ratios, particularly at 1:5 and 0:6, where the gold concentration rapidly decreased to 6.54 mg/L and 7.25 mg/L, respectively. This early-stage sorption reflects the high activity of the interpolymer system and the anion exchanger. Over time, the 4:2 ratio emerged as the most effective and selective for gold sorption. After 6 hours, the gold concentration dropped to 8.38 mg/L at this ratio, while iron slightly decreased to 18.3 mg/L, indicating a preference for gold. By the 48-hour mark, the 4:2 ratio exhibited the lowest residual gold concentration at 1.12 mg/L, while iron remained at 17.3 mg/L, demonstrating the system's efficiency and selectivity for gold. In comparison, the 1:5 ratio, despite high initial activity, showed less selectivity for gold, with residual concentrations of 1.42 mg/L for gold and 1.5 mg/L for iron after 48 hours. This indicates lower selectivity compared to the 4:2 ratio. These results suggest that the 4:2 ratio provides the optimal balance between effective sorption and selective recovery of gold over iron. Previous studies have shown that remote interactions between polyelectrolytes enhance ionization, improving sorption capacity for target ions.[63,64] In this study, the remote interaction between Amberlite IR120 and AV-17-8 in aqueous solution activated the ion exchangers, creating microenvironments conducive to gold binding. This enhanced ionization aligns with previous findings and contributes to the system's improved sorption efficiency.

Fig. 3 illustrates the sorption degree of gold and iron ions by the interpolymer system "Amberlite IR120H:AV-17-8" calculated using Equation 3. The evaluation of sorption efficiency provides critical insights into the system's performance and selectivity. At a 4:2 ratio, the system achieved a gold sorption efficiency of 96.26%, while iron sorption was lower at 42.33%, demonstrating strong selectivity for gold over 48 hours. The iron sorption efficiency was more than two times lower than that of gold. In contrast, the individual anion exchanger at a 0:6 ratio showed a gold sorption efficiency of 91.9%, indicating high sorption capacity. However, it also exhibited a high iron sorption efficiency of 92.33%, reflecting a lack of selectivity for gold.

3.2 Desorption of gold and iron ions from the AV-17-8 anion exchanger at different component ratios of the interpolymer system

The desorption behavior of aurum and iron ions is presented in Fig. 4, where the desorption degree R (Au, Fe) (%) was calculated using Equation (4). As shown in Fig. 4, the highest desorption of gold ions was observed at the 4:2 ratio, reaching 26.8 mg/L, corresponding to a desorption efficiency of 92.29%. This high efficiency aligns with the previously observed maximum sorption efficiency for gold ions at the same ratio, demonstrating a good correlation between the sorption and desorption processes. In contrast, the desorption efficiency for iron ions was significantly lower, with a maximum of 46.44% (5.9 mg/L) at the 4:2 ratio. The lower desorption of iron suggests stronger coordination with the functional groups of the interpolymer system compared to gold, reinforcing the system's selectivity for gold ions. Similarly, the individual anion exchanger at the 0:6 ratio showed a high gold desorption efficiency of 91.37% (25.2 mg/L) but exhibited less selectivity, with an iron desorption efficiency of 47.65% (13.2 mg/L).

3.3 Calculation and evaluation of the behavior of the interpolymer system per 1 mole of the structural unit of the AV-17-8 anion exchanger

The study aimed to calculate the sorption and desorption values per mole of the AV-17-8 anion exchanger across

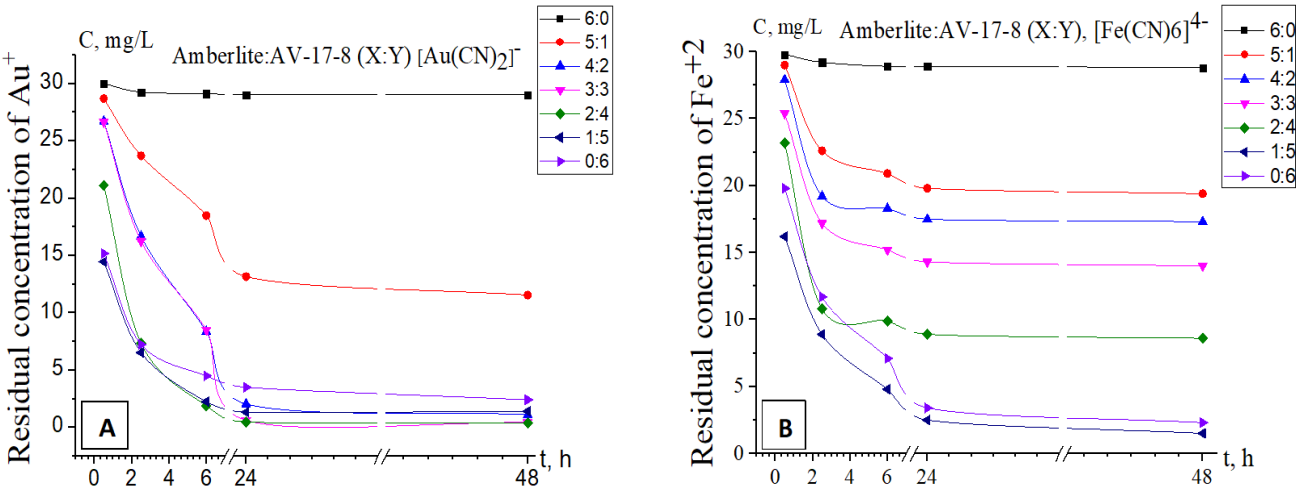

Fig. 2: The residual concentration (C) of (A) gold and (B) iron ions in solution after sorption as a function of time, conditions: temperature of 25 ºC.

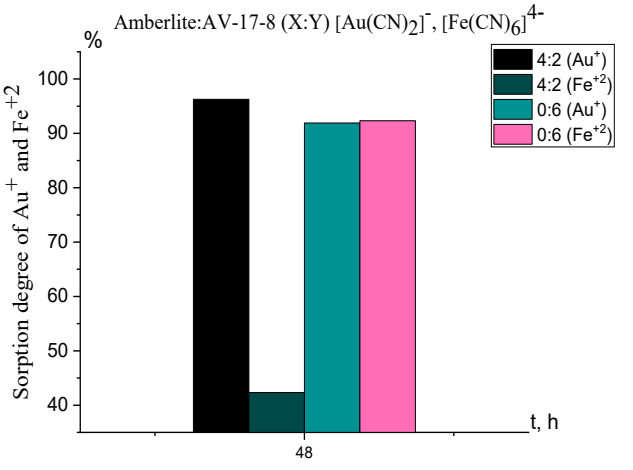

Fig. 3: The sorption degree of gold and iron ions by the interpolymer system "Amberlite IR120:AV-17-8" (4:2), as compared with the individual AV-17-8 (0:6) anion exchanger.

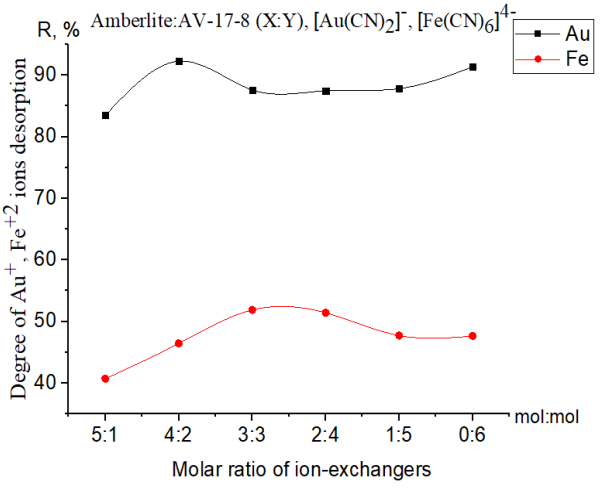

Fig. 4: The desorption behavior of gold and iron ions from the interpolymer system "Amberlite IR120:AV-17-8, conditions: temperature of 25 ºC.

different ratios of anion and cation exchangers in the interpolymer system. As shown in Fig. 5, reducing the proportion of the anion exchanger led to an increase in the amount of metal sorbed and desorbed per mole of the AV-17-8 unit. The highest gold sorption (18.45 mg/L) and desorption (15.4 mg/L) were observed at a 5:1 ratio, while these values decreased to 4.60 mg/L and 4.20 mg/L, respectively, at a 0:6 ratio, indicating more efficient utilization of the anion exchanger's active sites per mole. Similar trends were seen for iron ions. At a 5:1 ratio, iron sorption reached 10.60 mg/L, and desorption was 3.50 mg/L, while at a 0:6 ratio, these values dropped to 4.62 mg/L and 2.20 mg/L. Desorption from the cation exchanger was excluded due to negligible amounts of desorbed metal (0.02-0.035 mg/L). The ratio of anion to cation exchanger significantly affects the efficiency of gold and iron ion sorption and desorption. When calculated per mole of the anion exchanger, a lower proportion of the anion exchanger results in higher activity. However, the overall system's highest selectivity for gold ions is achieved at a 4:2 ratio. This enhanced selectivity is likely due to the optimal distribution of active sites and ionization of the system, creating favorable conditions for selective gold sorption.

3.4 Determination of the polymer chain binding degree

Based on Equation (5), the polymer chain binding degree (θ, %) of the interpolymer system "Amberlite IR120:AV-17-8" (X:Y) for Au(I) and Fe(II) ions was determined (Fig. 6). The results show a consistent increase in gold sorption across nearly all ratios, reflecting the system's effective binding capacity. After 48 hours, the highest binding degrees for gold were observed at ratios 4:2 and 2:4. In contrast, Fe(II) ions followed a different binding pattern. The 1:5 and 0:6 ratios exhibited the highest binding degrees for iron. At the 6:0 ratio, gold binding remained minimal at 0.7%, while iron binding was 2.9%. The comparative analysis indicates that, although the 1:5 and 0:6 ratios achieved the highest binding degrees for both gold and iron, the 4:2 ratio offers a more selective binding profile, with a clear preference for gold over iron.

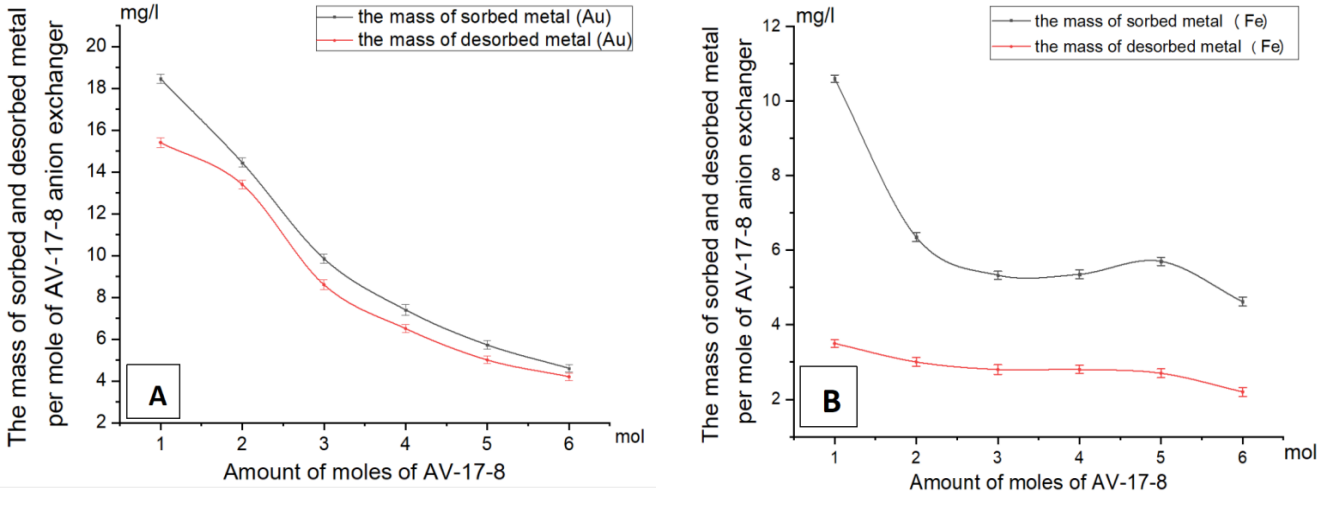

Fig. 5: Sorption and desorption of gold (A) and iron ions (B) per mole of AV-17-8 anion exchanger.

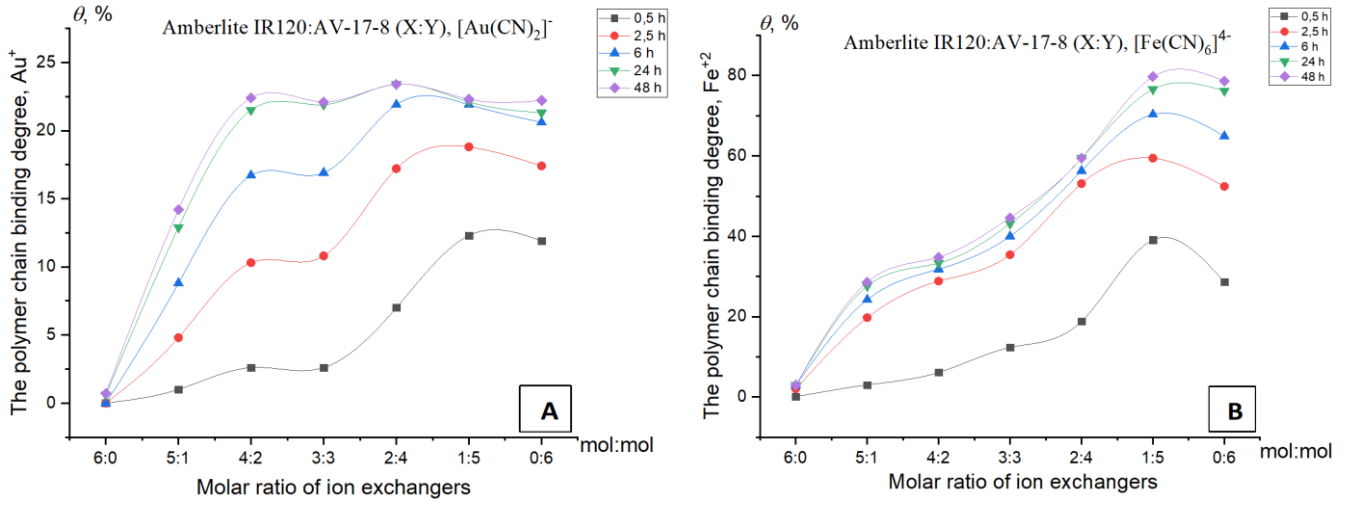

Fig. 6: The polymer chain binding degree of the interpolymer system "Amberlite IR120:AV-17-8" (Θ,%), regarding Gold ions (A) and Iron ions (B).

3.5 Determination of the effective dynamic exchange capacity (Q, mmol/g)

Based on Equation (6), the effective dynamic exchange capacity (Q) of the interpolymer system "Amberlite IR120:AV-17-8" (X:Y) for Au(I) and Fe(II) ions was determined (Fig. 7). In the initial stage of sorption (0.5 hours), the exchange capacity for gold ranged from 0 mmol/g at the 6:0 ratio to 0.657 mmol/g at the 1:5 ratio, while for iron, the highest exchange capacity reached 2.054 mmol/g at the same 1:5 ratio. As the sorption time increases, the exchange capacity for gold also increases, reaching 1.252 mmol/g at 4:2 ratio after 48 hours.

Fig. 8 represents the IR spectra of Amberlite IR120 before and after sorption and desorption, highlighting key spectral changes. The band at 3127.5 cm^{-1}, associated with hydrogen bonding of -SO_3H groups, shifts and splits into two distinct bands at 3385.2 cm^{-1} and 3211.1 cm^{-1} after sorption, indicating ionization and reorganization of the sulfonic acid groups.[65] The C-H stretching vibration remains stable, but the shift from 2410.3 cm^{-1} to 2425.3 cm^{-1} suggests an interaction with complex anions. The bands corresponding to sulfonic groups at 1124.8 cm^{-1}, 1038.3 cm^{-1}, and 1008.1 cm^{-1} also shift after sorption, confirming their involvement in the process. After desorption, the incomplete recovery of the polymer structure is indicated by a slight shift to 3390.7 cm^{-1}. Additionally, the disappearance of the 1269 cm^{-1} peak and changes in other key bands suggest partial restoration of functional groups and altered interactions within the polymer matrix after desorption.

Fig. 9 illustrates the IR spectra of the AV-17-8 (OH^-) anion exchange resin before and after the sorption and desorption of gold (Au) and iron (Fe) ions. The shift of the O–H stretching band from 3384.3 cm^{-1} to 3402.4 cm^{-1} after sorption suggests hydrogen bonding rearrangements. The appearance of newbands at 2141.8 cm^{-1}, 2109.5 cm^{-1}, and 2044.4 cm^{-1} confirms the formation of gold-cyanide complexes such as

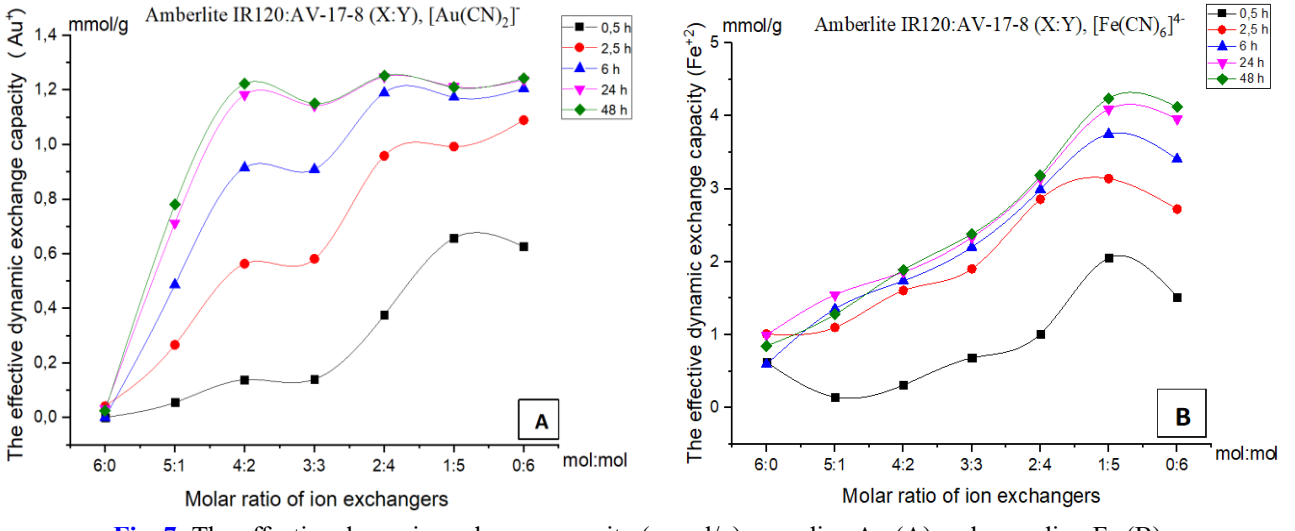

Fig. 7: The effective dynamic exchange capacity (mmol/g) regarding Au (A) and regarding Fe (B).

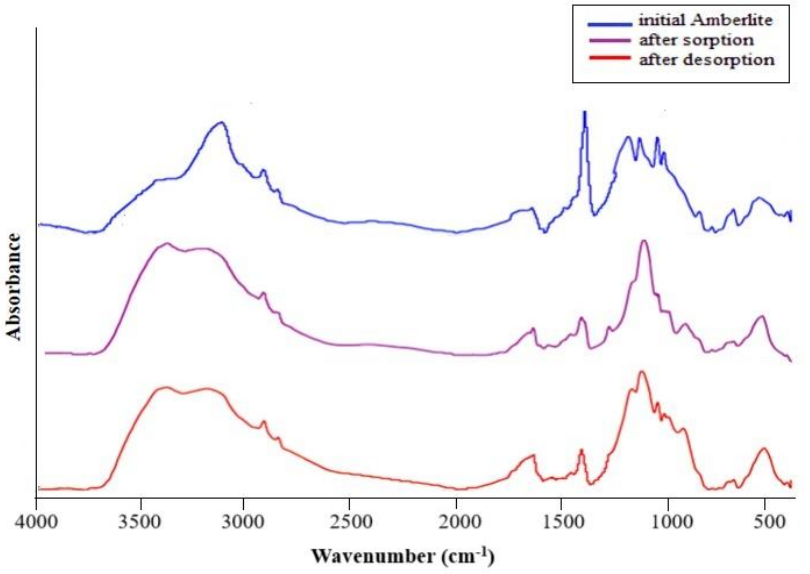

Fig. 8: FTIR spectra of initial Amberlite IR120, Amberlite IR120 (4:2) after sorption, and Amberlite IR120 (4:2) after desorption process.

$[Au(CN)_2]^-$ and $[Fe(CN)_6]^{4-}$. After desorption, partial recovery of the resin structure is evident from the shift of the O–H/N–H band to 3389.9 cm^{-1}, while the C–H stretching vibrations remain unchanged, indicating the preservation of aliphatic chains. A new band at 2068.9 cm^{-1}, likely due to residual nitrile groups or metal complexes, further confirms incomplete desorption. Overall, the results demonstrate the resin's capability for repeated sorption-desorption cycles with maintained structural integrity.

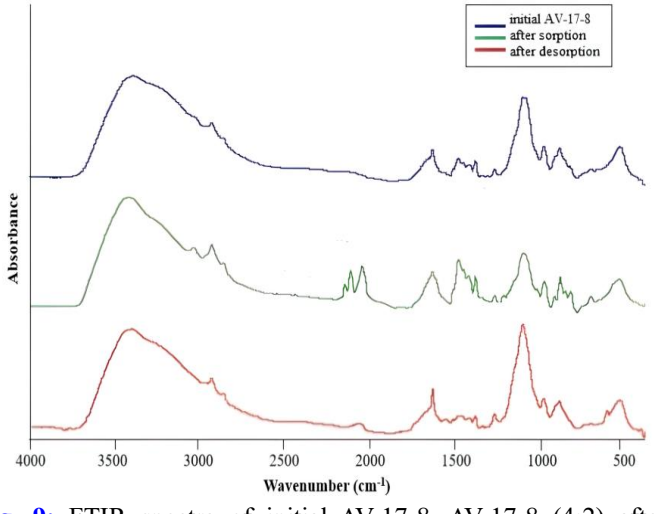

Fig. 9: FTIR spectra of initial AV-17-8, AV-17-8 (4:2) after sorption, and AV-17-8 (4:2) after desorption process.

3.6 TGA of the interpolymer system "Amberlite IR120:AV-17-8" (4:2)

The TGA a result for Amberlite IR120, both before and after the sorption process, are shown in Fig. 10. Thermogravimetric analysis of Amberlite IR120 was conducted in the temperature range of 0-600 °C at a heating rate of 10 °C/min under an inert atmosphere, both before and after the sorption of Au^+ and Fe^{2+} ions. For the sample before sorption, an initial mass loss of about 10% occurs between 50 and 125 °C, mainly due to the removal of moisture and volatile compounds. By 250 °C, the total loss reaches ~15%. Intensive degradation in the 250-350 °C range raises the loss to ~40%, and further decomposition between 350 and 450 °C increases it to ~80%. At 600 °C, approximately 17% of the initial mass remains. In contrast, the sample after sorption shows only a ~5% mass loss between 50 and 125 °C, increasing to ~10% by 250 °C. Between 250 and 350 °C, the total loss reaches ~30%. Further degradation between 350 and 450 °C raises the overall loss to ~55%. By 600 °C, approximately 40% of the initial mass remains.

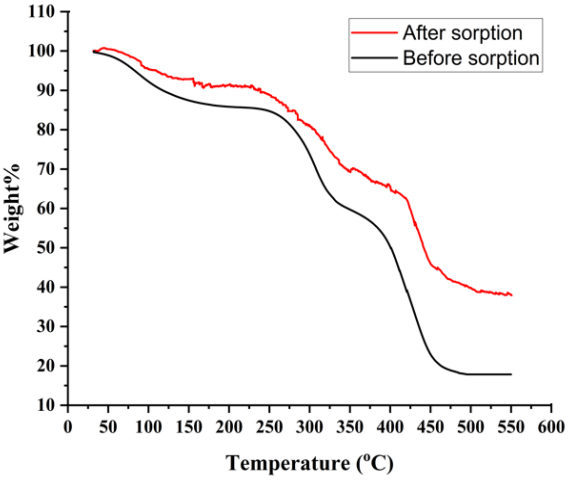

Fig. 10: TGA of initial Amberlite IR120 and Amberlite IR120 from the interpolymer system "Amberlite IR120:AV-17-8" (4:2).

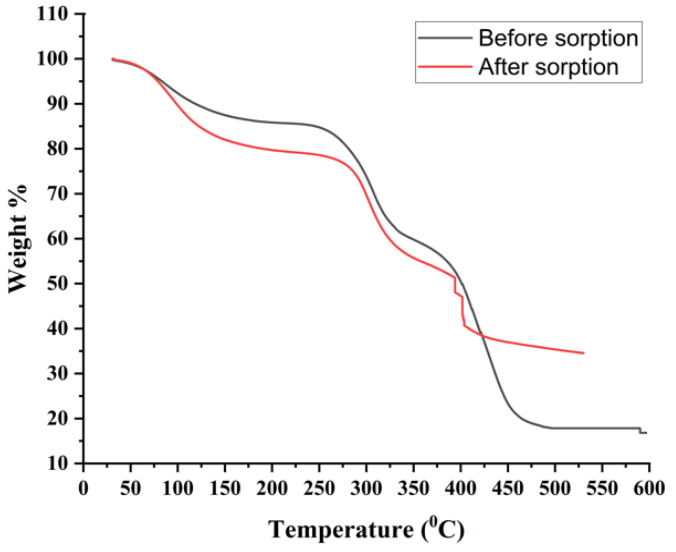

Fig. 11: TGA of initial AV-17-8 and AV-17-8 from the interpolymer system "Amberlite IR120:AV-17-8" (4:2).

The TGA results for AV-17-8 are shown in Fig. 11. For the sample before sorption, an initial 10% mass loss occurs between 50-150 °C. This loss increases to 15% by 250 °C and reaches approximately 40% by 350 °C. Degradation continues up to 500 °C, where total mass loss is 85%, leaving only about 15% of the initial mass at 600 °C. The sample after sorption shows a 20% loss in the 50-150 °C range. By 250 °C, cumulative losses rise to 25% and reach about 45% by 350 °C. Between 350 and 450 °C, degradation increases total losses to 65%, and approximately 32% of the initial mass remains at 550 °C.

3.6 SEM of the interpolymer system "Amberlite IR120:AV-17-8" (4:2)

Fig. 12 represents the SEM and EDS analysis of the Amberlite IR120 sample before and after the sorption process. In the initial SEM image, the surface of the Amberlite resin appears relatively smooth, with visible elements primarily consisting of carbon, oxygen, and sulfur, which align with its sulfonated polystyrene structure and functional sulfonic acid groups (-SO_3H). The EDS spectrum shows prominent peaks corresponding to these elements, indicating the typical composition of the resin before metal ion sorption. Post-sorption analysis identified trace amounts of metals, including iron (0.30%) and gold (1.05%), indicating partial uptake of these metals.

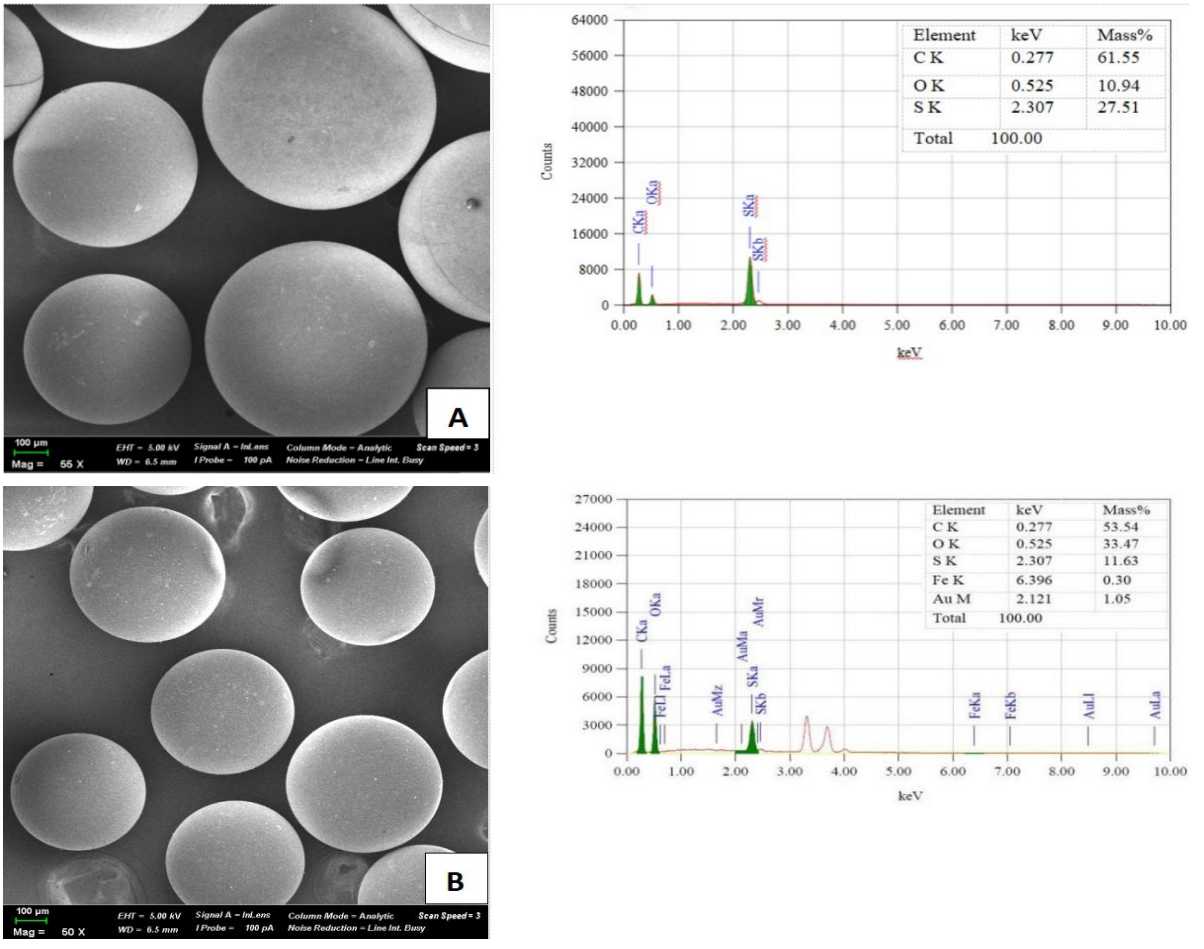

Fig. 12: SEM and EDS of initial Amberlite IR120 (A) and Amberlite IR120 from the interpolymer system "Amberlite IR120:AV-17-8" (4:2) (B).

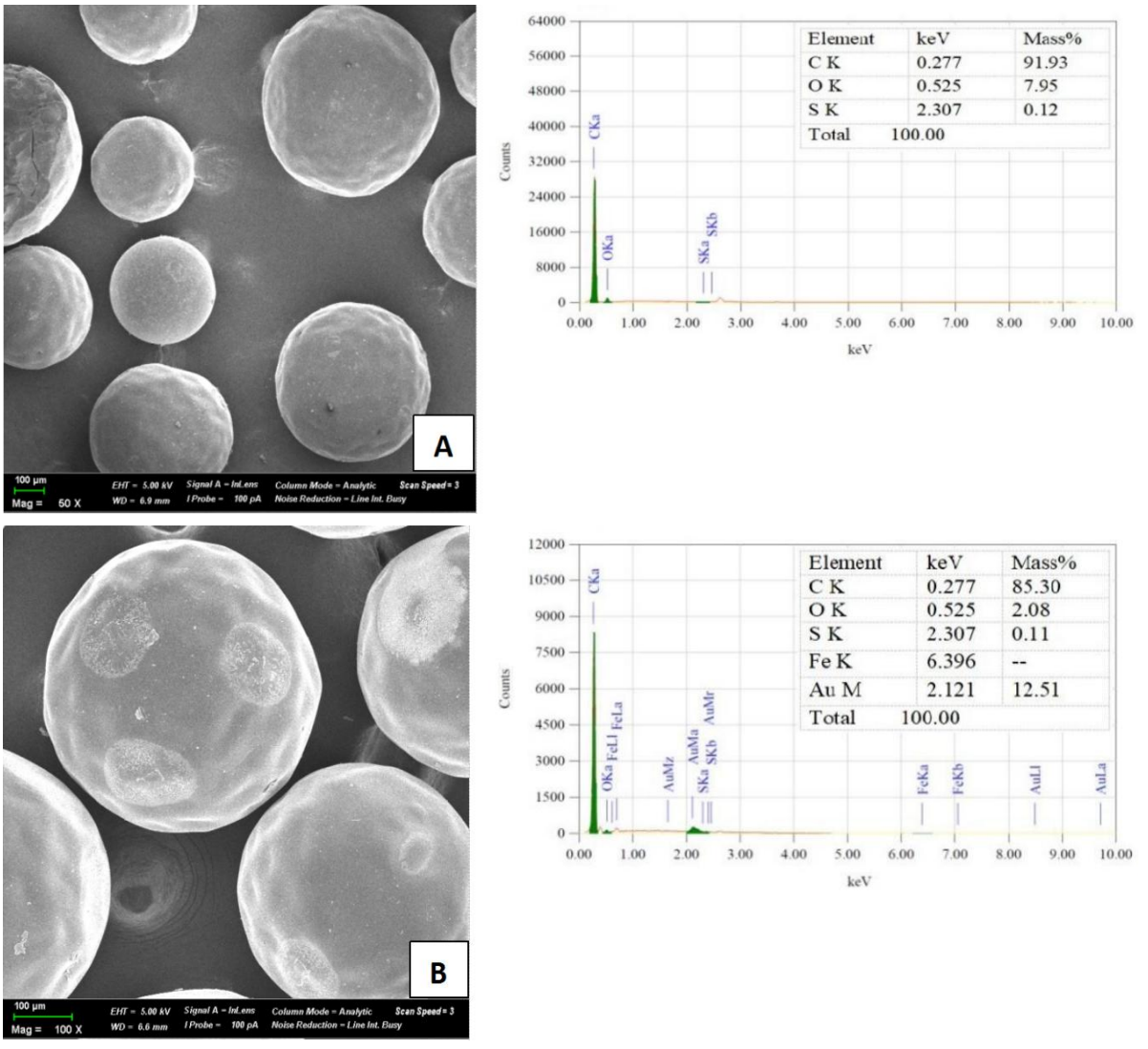

Fig. 13: SEM and EDS of initial AV-17-8 (A) and AV-17-8 from the interpolymer system "Amberlite IR120:AV-17-8" (4:2) (B).

Fig. 13 presents the SEM and EDS analyses of the AV-17-8 anion exchanger before and after the sorption process. SEM images of the initial AV-17-8 state show a smooth, homogeneous surface, with EDS confirming the composition of carbon (91.93%) and oxygen (7.95%). After sorption, the surface becomes rough with visible clusters, indicating metal binding. Gold content reaches 12.51%, while iron is not detected, demonstrating high selectivity. The reduction in carbon and oxygen suggests the involvement of functional groups in ion exchange.

4. Conclusion

This research presents a comprehensive evaluation of the interpolymer system "Amberlite IR120: AV-17-8" for the selective sorption of gold ions from complex solutions containing both gold and iron ions. The optimal ratio of 4:2 demonstrated a high gold sorption efficiency of 96.26% after 48 hours while limiting iron sorption to 42.33%, emphasizing the system's selectivity for gold ions. The study confirmed that the remote interaction between Amberlite IR120 (H^+ form) and AV-17-8 (OH^- form) enhances ion exchange through the activation and stabilization of functional groups, supported by Pearson's HSAB theory. These interactions significantly improved the selective sorption of gold ions. Desorption experiments using 9% thiourea and 2% sulfuric acid achieved 92.28% gold desorption, further highlighting the system's efficiency in selectively recovering gold ions. This work establishes a foundation for further research into the system's scalability, process optimization, and economic feasibility. Future studies should focus on process parameter optimization, regeneration capability, and performance under varying conditions to extend the technology's applicability to other valuable metals such as platinum, palladium, silver, and rare earth metals. In conclusion, the "Amberlite IR120:AV-17-8" interpolymer system, particularly at a 4:2 ratio, presents a promising and efficient solution for the selective sorption of gold ions, offering significant potential for large-scale applications and future industrial development.

Acknowledgement
This research has been funded by the Science Committee of the Ministry of Science and Higher Education of the Republic of Kazakhstan, grant number BR18574042.

Conflict of Interest
There is no conflict of interest.

Supporting Information
Not applicable.

References
[1] K. Kongolo, M. D. Mwema, The extractive metallurgy of gold, *Hyperfine Interactions*, 1998, **111**, 281-289, doi: 10.1023/A:1012678306334.
[2] J. Schwank, Gold in bimetallic catalysts, *Gold Bulletin*, 1985, **18**, 2-10, doi: 10.1007/BF03214680.
[3] C. W. Corti, R. J. Holliday, Commercial aspects of gold applications: from materials science to chemical science, *Gold Bulletin*, 2004, **37**, 20-26, doi: 10.1007/BF03215513.
[4] C. Milone, R. Ingoglia, S. Galvagno, Gold supported on iron oxy-hydroxides: a versatile tool for the synthesis of fine chemicals, *Gold Bulletin*, 2006, **39**, 54-65, doi: 10.1007/BF03215277.
[5] M. D. Rao, K. K. Singh, C. A. Morrison, J. B. Love, Challenges and opportunities in the recovery of gold from electronic waste, *RSC Advances*, 2020, **10**, 4300-4309, doi: 10.1039/C9RA07607G.
[6] D. Medina, C. G. Anderson, A review of the cyanidation treatment of copper-gold ores and concentrates, *Metals*, 2020, **10**, 897, doi: 10.3390/met10070897.
[7] D. M. Muir, A review of the selective leaching of gold from oxidised copper-gold ores with ammonia-cyanide and new insights for plant control and operation, *Minerals Engineering*, 2011, **24**, 576-582, doi: 10.1016/j.mineng.2010.08.022.
[8] Z. Liu, X. Guo, Q. Tian, L. Zhang, A systematic review of gold sorption: fundamentals, advancements, and challenges toward alternative lixiviants, *Journal of Hazardous Materials*, 2022, **440**, 129778, doi: 10.1016/j.jhazmat.2022.129778.
[9] A. Yoshimura, K. Takatori, Y. Matsuno, environmentally sound recovery of gold from waste electrical and electronic equipment using organic aqua regia, *International Journal of Automation Technology*, 2020, **14**, 999-1004, doi: 10.20965/ijat.2020.p0999.
[10] Z. Sun, Y. Xiao, J. Sietsma, H. Agterhuis, Y. Yang, A cleaner process for selective recovery of valuable metals from electronic waste of complex mixtures of end-of-life electronic products, *Environmental Science & Technology*, 2015, **49**, 7981-7988, doi: 10.1021/acs.est.5b01023.
[11] M. Kunarbekova, Y. Yeszhan, S. Zharylkan, M. Alipuly, U. Zhantikeyev, A. Beisebayeva, K. Kudaibergenov, K. Rysbekov, Z. Toktarbay, S. Azat, The state of the art of the mining and metallurgical industry in Kazakhstan and future perspectives: a systematic review, *ES Materials & Manufacturing*, 2024, **25**, 1219, doi: 10.30919/esmm1219.
[12] W. Jin, Y. Zhang, Sustainable electrochemical extraction of metal resources from waste streams: From removal to recovery, *ACS Sustainable Chemistry & Engineering*, 2020, **8**, 4693-4707, doi: 10.1021/acssuschemeng.9b07007.
[13] A. Laplante, S. Gray, Advances in gravity gold technology, *Developments in Mineral Processing*, 2005, **15**, 280-307, doi: 10.1016/S0167-4528(05)15013-3.
[14] A. R. Laplante, F. Woodcock, M. Noaparast, Predicting gravity separation gold recoveries, *Mining, Metallurgy & Exploration*, 1995, **12**, 74-79, doi: 10.1007/BF03403081.
[15] R. Dunne, Flotation of gold and gold-bearing ores, Gold Ore Processing, Elsevier, Amsterdam, 2016, 315-338, ISBN: 978-0-444-63658-4.
[16] A. Gül, O. Kangal, A. A. Sirkeci, G. Önal, Beneficiation of the gold bearing ore by gravity and flotation, *International Journal of Minerals, Metallurgy, and Materials*, 2012, **19**, 106-110, doi: 10.1007/s12613-012-0523-4.
[17] A. Falconer, Gravity separation: old technique/new methods, *Physical Separation in Science and Engineering*, 2003, **12**, 31-48, doi: 10.1080/1478647031000104293.
[18] C. A. Barbu, N. Tomuș, A. D. Radu, M. Zlăgnean, I. C. Popescu, Gravity separation: highly effective tool for gold-bearing slag's recycling, *Journal of Sustainable Metallurgy*, 2021, **7**, 1852-1861, doi: 10.1007/s40831-021-00458-9.
[19] S. Azat, E. Arkhangelsky, T. Papathanasiou, A. Zorpas, A. Abirov, V. Inglezakis, Synthesis of biosourced silica-Ag nanocomposites and amalgamation reaction with mercury in aqueous solutions, *Comptes Rendus Chimie*, 2020, **23**, 77-92, doi: 10.5802/crchim.19.
[20] V. J. Inglezakis, S. Azat, Z. Tauanov, S. V. Mikhalovsky, Functionalization of biosourced silica and surface reactions with mercury in aqueous solutions, *Chemical Engineering Journal*, 2021, **423**, 129745, doi: 10.1016/j.cej.2021.129745.
[21] A. K. Donkor, H. Ghoveisi, J. J. Bonzongo, Use of metallic mercury in artisanal gold mining by amalgamation: A review of temporal and spatial trends and environmental pollution, *Minerals*, 2024, **14**, 555, doi: 10.3390/min14060555.
[22] F. Alguacil, The chemistry of gold sorption, The Chemistry of Gold Extraction, Society for Mining, Metallurgy and Exploration, Littleton, 2006, 297-364, ISBN: 978-0-87335-240-6.
[23] T. J. Manning, D. W. Kappes, Heap leaching of gold and silver ores, Gold Ore Processing, Elsevier, Amsterdam, 2016, 413-428, ISBN: 978-0-444-63658-4.
[24] J. Petersen, Heap leaching as a key technology for recovery of values from low-grade ores-a brief overview, *Hydrometallurgy*, 2016, **165**, 206-212, doi: 10.1016/j.hydromet.2015.09.001.
[25] T. Thenepalli, R. Chilakala, L. Habte, L. Q. Tuan, C. S. Kim, A brief note on the heap leaching technologies for the recovery of valuable metals, *Sustainability*, 2019, **11**, 3347, doi: 10.3390/su11123347.
[26] Y. Kita, H. Nishikawa, T. Takemoto, Effects of cyanide and dissolved oxygen concentration on biological Au recovery,

Journal of Biotechnology, 2006, **124**, 545-551, doi: 10.1016/j.jbiotec.2006.01.038.
[27] Y. A. Attia, M. El-Zeky, Bioleaching of gold pyrite tailings with adapted bacteria, *Hydrometallurgy*, 1989, **22**, 291-300, doi: 10.1016/0304-386X(89)90026-1.
[28] D. Shin, J. Jeong, S. Lee, B. D. Pandey, J. C. Lee, Evaluation of bioleaching factors on gold recovery from ore by cyanide-producing bacteria, *Minerals Engineering*, 2013, **48**, 20-24, doi: 10.1016/j.mineng.2013.03.019.
[29] E. Jorjani, H. Askari Sabzkoohi, Gold leaching from ores using biogenic lixiviants-a review, *Current Research in Biotechnology*, 2022, **4**, 10-20, doi: 10.1016/j.crbiot.2021.12.003.
[30] M. Gökelma, A. Birich, S. Stopic, B. Friedrich, A review on alternative gold recovery reagents to cyanide, *Journal of Materials Science and Chemical Engineering*, 2016, **4**, 8-17, doi: 10.4236/msce.2016.48002.
[31] M. C. Laker, Environmental impacts of gold mining: with special reference to South Africa, *Mining*, 2023, **3**, 205-220, doi: 10.3390/mining3020012.
[32] J. Kim, R. Kim, K. N. Han, Advances in hydrometallurgical gold recovery through cementation, adsorption, ion exchange and solvent extraction, *Minerals*, 2024, **14**, 607, doi: 10.3390/min14060607.
[33] D. B. Donato, O. Nichols, H. Possingham, M. Moore, P. F. Ricci, B. N. Noller, A critical review of the effects of gold cyanide-bearing tailings solutions on wildlife, *Environment International*, 2007, **33**, 974-984, doi: 10.1016/j.envint.2007.04.007.
[34] A. Birich, S. Stopic, B. Friedrich, Kinetic investigation and dissolution behavior of cyanide alternative gold leaching reagents, *Scientific Reports*, 2019, **9**, 7191, doi: 10.1038/s41598-019-43383-4.
[35] E. Neag, E. Kovacs, Z. Dinca, A. Iulia Török, C. Varaticeanu, E. Andrea Levei, Hydrometallurgical recovery of gold from mining wastes, Strategies of Sustainable Solid Waste Management, IntechOpen, London, 2021, 108-121, ISBN: 978-1-83962-560-2.
[36] H. Wan, J. Qu, L. Zhao, X. Bu, Improving the flotation performance of fine molybdenite using superhydrophobic magnetic carriers, *Minerals Engineering*, 2025, **224**, 109212, doi: 10.1016/j.mineng.2025.109212.
[37], N. Kydyrbay, E. Adotey, M. Zhazitov, Z. Suiindik, Z. Toktarbay, N. Nuraje, O. Toktarbaiuly, Enhancing road durability and safety: A study on silica-based superhydrophobic coating for cement surfaces in road construction, *Engineered Science*, 2024, **30,** 1221, doi: 10.30919/es1221.
[38] Z. Suiindik, E. Adotey, N. Kydyrbay, M. Zhazitov, N. Nuraje, Formulating superhydrophobic coatings with silane for microfiber applications, *Eurasian Chemico-Technological Journal*, 2024, **26**, 53-60, doi: 10.18321/ectj1607.
[39] O. Toktarbaiuly, A. Kurbanova, G. Imekova, M. Abutalip, Z. Toktarbay, Desert water saving and transportation for enhanced oil recovery: bridging the gap for sustainable oil recovery, *Eurasian Chemico-Technological Journal*, 2023, **25**, 193-200, doi: 10.18321/ectj1522.
[40] T. K. Jumadilov, Z. B. Malimbayeva, K. Khimersen, I. S. Saparbekova, A. M. Imangazy, O. V. Suberlyak, L. P. N. University, Specific features of praseodymium extraction by intergel system based on polyacrylic acid and poly-4-vinylpyridine hydrogels, *Bulletin of the Karaganda University "Chemistry" Series*, 2021, **103**, 53-59, doi: 10.31489/2021ch3/53-59.
[41] G. Zhou, C. Liu, L. Chu, Y. Tang, S. Luo, Rapid and efficient treatment of wastewater with high-concentration heavy metals using a new type of hydrogel-based adsorption process, *Bioresource Technology*, 2016, **219**, 451-457, doi: 10.1016/j.biortech.2016.07.038.
[42] T. Jumadilov, B. Totkhuskyzy, A. Imangazy, J. Gražulevičius, Anomalous sorption of yttrium ions by the mutual activated hydrogels in the interpolymer system of poly(methacrylic acid) and poly(4-vinylpyridine), *Chemistry & Chemical Technology*, 2023, **17**, 52-59, doi: 10.23939/chcht17.01.052.
[43] T. K. Jumadilov, A. M. Imangazy, K. Khimersen, J. T. Haponiuk, Remote interaction effect of industrial ion exchangers on the electrochemical and sorption equilibrium in scandium sulfate solution, *Polymer Bulletin*, 2024, **81**, 2023-2041, doi: 10.1007/s00289-023-04800-x.
[44] T. Jumadilov, A. Utesheva, J. Grazulevicius, A. Imangazy, Selective sorption of cerium ions from uranium-containing solutions by remotely activated ion exchangers, *Polymers*, 2023, **15**, 816, doi: 10.3390/polym15040816.
[45] A. Imangazy, T. Jumadilov, K. Khimersen, A. Bayshibekov, Enhanced sorption of europium and scandium ions from nitrate solutions by remotely activated ion exchangers, *Polymers*, 2023, **15**, 1194, doi: 10.3390/polym15051194.
[46] D. A. Msumange, E. Y. Yazici, C. Oktay, D. Hacı, K. Aleksei, K. Kirill, Recovery of Au and Ag from the roasted calcine of a copper-rich pyritic refractory gold ore using ion exchange resins, *Minerals Engineering*, 2023, **195**, 108017, doi: 10.1016/j.mineng.2023.108017.
[47] K. Kudpeng, T. Bohu, C. Morris, P. Thiravetyan, A. H. Kaksonen, Bioleaching of gold from sulfidic gold ore concentrate and electronic waste by Roseovarius tolerans and Roseovarius mucosus, *Microorganisms*, 2020, **8**, 1783, doi: 10.3390/microorganisms8111783.
[48] H. Qin, T. Hu, Y. Zhai, N. Lu, J. Aliyeva, The improved methods of heavy metals removal by biosorbents: A review, *Environmental Pollution*, 2020, **258**, 113777, doi: 10.1016/j.envpol.2019.113777.
[49] X. Liu, Q. Hu, Z. Fang, X. Zhang, B. Zhang, Magnetic chitosan nanocomposites: a useful recyclable tool for heavy metal ion removal, *Langmuir*, 2009, **25**, 3-8, doi: 10.1021/la802754t.
[50] U. Upadhyay, I. Sreedhar, S. A. Singh, C. M. Patel, K. L. Anitha, Recent advances in heavy metal removal by chitosan based adsorbents, *Carbohydrate Polymers*, 2021, **251**, 117000, doi: 10.1016/j.carbpol.2020.117000.
[51] A. Tapfuma, D. P. Chakawa, L. B. Moyo, N. Hlabangana, G. Danha, E. Muzenda, Investigating the feasibility of using agricultural waste as an adsorbent of gold ions in small scale gold processing plants, *Procedia Manufacturing*, 2019, **35**, 85-90, doi:

10.1016/j.promfg.2019.05.008.
[52] M. Barczak, K. Michalak-Zwierz, K. Gdula, K. Tyszczuk-Rotko, R. Dobrowolski, A. Dąbrowski, Ordered mesoporous carbons as effective sorbents for removal of heavy metal ions, *Microporous and Mesoporous Materials,* 2015, **211**, 162-173, doi: 10.1016/j.micromeso.2015.03.010.
[53] M. D. Adams, The mechanisms of adsorption of $Ag(CN)_2^-$ and Ag+ on to activated carbon, *Hydrometallurgy*, 1992, **31**, 121-138, doi: 10.1016/0304-386X(92)90112-D.
[54] A. Akhmetzhan, N. Abeu, S. N. Longinos, A. Tashenov, N. Myrzakhmetova, N. Amangeldi, Z. Kuanyshova, Z. Ospanova, Z. Toktarbay, Synthesis and heavy-metal sorption studies of N, N-dimethylacrylamide-based hydrogels, *Polymers*, 2021, **13**, 3084, doi: 10.3390/polym13183084.
[55] A. Akhmetzhan, N. Myrzakhmetova, N. Amangeldi, Z. Kuanyshova, N. Akimbayeva, S. Dosmaganbetova, Z. Toktarbay, S. N. Longinos, A short review on the N, N-dimethylacrylamide-based hydrogels, *Gels*, 2021, **7**, 234, doi: 10.3390/gels7040234.
[56] E. Jorjani, H. Askari Sabzkoohi, Gold leaching from ores using biogenic lixiviants-a review, *Current Research in Biotechnology*, 2022, **4**, 10-20, doi: 10.1016/j.crbiot.2021.12.003.
[57] D. Mishra, D. J. Kim, D. E. Ralph, J. G. Ahn, Y. H. Rhee, Bioleaching of metals from spent lithium ion secondary batteries using Acidithiobacillus ferrooxidans, *Waste Management*, 2008, **28**, 333-338, doi: 10.1016/j.wasman.2007.01.010.
[58] C. A. Fleming, Hydrometallurgy of precious metals recovery, *Hydrometallurgy*, 1992, **30**, 127-162, doi: 10.1016/0304-386x(92)90081-a.
[59] C. Ocampo-López, L. Rendón-Castrillón, M. Ramírez-Carmona, F. González-López, Evaluation of the preg-robbing effect in gold recovery using the carbon-in-leach technique: A comparative study of three reactor types, *Metals*, 2024, **14**, 1465, doi: 10.3390/met14121465.
[60] S. C. S. Ramli, R. Mohd Osman, Meeting the challenge of Penjom Gold Mine's geology in the recovery of fine gold in carbonaceous ores, *Bulletin of the Geological Society of Malaysia*, 2015, **61**, 1-9, doi: 10.7186/bgsm61201501.
[61] A. Alfarra, E. Frackowiak, F. Béguin, The HSAB concept as a means to interpret the adsorption of metal ions onto activated carbons, *Applied Surface Science*, 2004, **228**, 84-92, doi: 10.1016/j.apsusc.2003.12.033.
[62] R. G. Pearson, Hard and soft acids and bases, *Journal of the American Chemical Society*, 1963, **85**, 3533-3539, doi: 10.1021/ja00905a001.
[63] T. Jumadilov, K. Khuangul, J. Haponiuk, Influence of initial states on the electrochemical behavior of industrial ionites in the interpolymer system Lewatit CNPLF-AV-17-8, Advanced Polymer Structures: Chemistry for Engineering Applications, Apple Academic Press, Waretown, 2023, 83-95, ISBN: 978-1-77491-301-7.
[64] T. Jumadilov, K. Khimersen, J. Haponiuk, B. Totkhuskyzy, Enhanced lutetium ion sorption from aqueous solutions using activated ion exchangers, *Polymers*, 2024, **16**, 220, doi: 10.3390/polym16020220.
[65] E. Pretsch, P. Bühlmann, M. Badertscher, Structure determination of organic compounds, Berlin Heidelberg: Springer, 2020, ISBN: 978-3-662-62438-8.